ELSEVIER

Journal of Non-Crystalline Solids 247 (1999) 1–8

JOURNAL OF NON-CRYSTALLINE SOLIDS

Section 1. Oxide glasses and nanocomposites

An approach to new glasses through phase separation

Satoru Inoue [a,*], Akio Makishima [b], Hiroyuki Inoue [b], Kohei Soga [b], Tomoya Konishi [b], Tomoyoshi Asano [b]

[a] *National Institute for Research in Inorganic Materials, Namiki 1-1, Tsukuba, Ibaraki 305-0044, Japan*

[b] *Department of Materials Science, School of Engineering, The University of Tokyo, 3-1, Hongo 7-chome, Bunkyo-ku, Tokyo 113-0033, Japan*

Abstract

The application of liquid–liquid phase separation to the preparation of new glasses has been demonstrated. The in situ observation of phase separation has been made on some borate liquids at 1-*g* (*g* ≡ gravitational field at Earth's surface) and under microgravity circumstances (drop tests) to estimate rates of phase separation. The liquid–liquid phase separation of barium borate liquids resulted in the precipitation of droplets of several tens of a micrometer in diameter, which was assumed to be applicable for the preparation of glass spheres, lens array, etc. The addition of rare earth oxide to the systems resulted in enriching the rare earth content of the precipitated droplets, indicating that the composition of the droplets would be modified by adding another oxide to melts. The microgravity circumstances decreased the phase separation rates and were found to be favorable for the preparation of glass spheres.

1. Introduction

The binary borate systems such as $MgO–B_2O_3$, $CaO–B_2O_3$, $SrO–B_2O_3$, $BaO–B_2O_3$, $PbO–B_2O_3$ and the silicate systems such as $BaO–SiO_2$, $SrO–SiO_2$, $FeO–Fe_2O_3–SiO_2$ have liquid–liquid phase separation phenomena in which the uniform liquid decomposes into two liquids in the temperature range between the critical temperature (T_c, the immiscibility temperature) and the liquidus temperature (T_l) [1]. In the case that the minor phase possesses a surface tension larger than that of the residual major phase, the minor phase is precipitated as droplets in the residual liquid [2]. Phase separation is a phenomena applicable to prepare glasses with dispersed glassy or crystalline particles, giving the glasses unique properties or functions. For example, the phase separation in the $Na_2O–B_2O_3–SiO_2$ system has been applied to prepare porous glasses [3], anisotropic glasses [4], and non-linear optic glasses [5].

In applying phase separation to the preparation of unique materials, it is important to freeze the texture of the system when the separated particles grow to an appropriate size. For this purpose, it is necessary to know the phase separation rate or, if possible, the nucleation rate, and the growth rate in the system of interest.

The convection, the floating force and the static pressure are derived from the gravity at 1-*g* in the liquids. Convection would change the concentration profiles of the diffusing ions and affect the phase separation rate [6]. The existence of floating force might interfere with the uniform distribution of the droplets and the static pressure might distort

* Corresponding author. E-mail: inoues@nirim.go.jp

0022-3093/99/$ – see front matter
PII: S0022-3093(99)00081-2

the spherical shapes of the droplets. Therefore we expect microgravity environments to give a uniform dispersion of spherical droplets in the liquid–liquid phase separation, leading to textures favorable for the preparation of composite materials. From the view points of research on stable phase separation, the ideal concentration profiles of the diffusing ions would provide the basic and important understanding of the mechanisms of stable phase separation.

In this study, the application of liquid–liquid phase separation to the preparation of new glasses has been demonstrated with a review of the in situ observation of phase separation made on some borate liquids at 1-*g* and under microgravity circumstances (drop tests) [7–9].

2. Experimental

2.1. Approach to new glasses

Fig. 1 shows the schematic illustration of the processes for the approach to preparing glasses by utilizing the phase separation. The phase separation takes place between T_c and T_l. The traces of the critical temperatures as a function of the melt composition correspond to the immiscibility temperature curves, which are given in the phase diagrams [10].

The melt is heated to a temperature greater than T_c to become uniform and is then cooled to an appropriate phase separation temperature (T_p) between T_c and T_l with various cooling programs. The phase separation initiates by nucleation and proceeds by the growth of the nuclei to droplets of appropriate sizes. After the heat treatment for the phase separation, the melt is cooled at a rate sufficient to freeze the texture of the liquid, giving phase separated glasses at room temperature. The textures of the phase separated glasses, the sizes and the volume fraction of the droplets, are controlled by the composition of the melt, the phase separation temperature, T_p, and the cooling schedule. The addition of a rare earth oxide to the system might change the composition of the droplets, resulting in the enrichment of the rare earth ion content of droplet [11]. The sizes of the droplets could be controlled in the range from several tens of a nanometer to several tens of a micrometer [2].

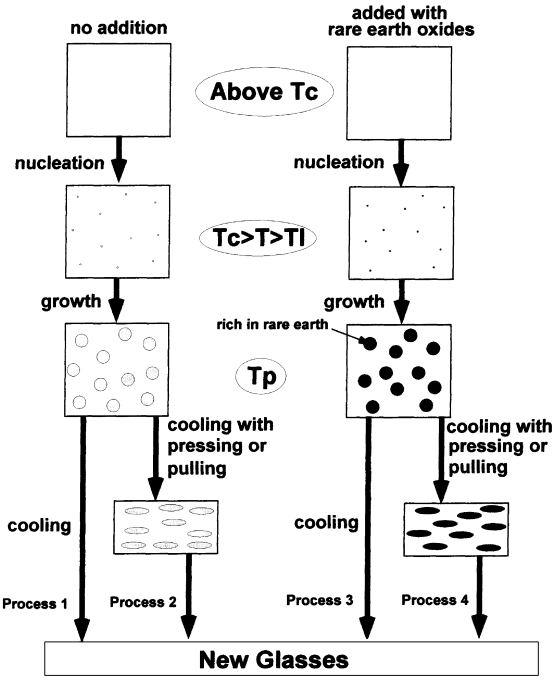

Fig. 1. Processes for the approach to new glasses through phase separation.

Our Process 1 gives glasses with dispersed glassy or crystalline spherical particles. The glasses obtained in Process 3 are assumed to be similar to the products from Process 1, but the compositions of the droplets differ.

In Processes 2 and 4, the melts were pressed or spread during cooling, resulting in the collapse of the droplets. The products are the glasses containing dispersed elliptical droplets, giving unique glasses which are anisotropic in some properties such as optical properties, electrical properties, and magnetic properties. Moreover these glasses properly prepared could be applicable to second order non-linear optic glasses.

2.2. Phase separation rate at 1-g

The author and colleagues investigated the separation rates of the liquid–liquid phase separation in $PbO–B_2O_3$ [7] and $BaO–B_2O_3$ [8] system

by applying an in situ observation technique. The block diagram of the set up for the in situ observation of phase separation is given in Fig. 2. The sample glass of ~0.18 g for $PbO–B_2O_3$ system and ~0.5 g for $BaO–B_2O_3$ system was placed in a platinum pan (13 mm in diameter) and was remelted in an electric furnace at an appropriate temperatures above T_c to get an homogeneous liquid. The phase separation was observed by a video camera continuously as the liquid was cooled from the homogenization temperature at a rate of 2.5°C/min. The pictures were recorded on a video tape. The size of the visual field was 590×801 μm^2 and the magnification on a TV-monitor (14 in.) was 357×. Fig. 3 shows the pictures taken on the PbO–and BaO–borate melts. In $PbO–B_2O_3$ system, the picture observed became dark due to the light scattering when the droplets precipitated. For $PbO–B_2O_3$ system, the time interval, t, between the beginning and the completion of the darkening of the central 500×700 μm^2 area within the visual field, was determined as the measure of the phase separation rate. In $BaO–B_2O_3$ system, the droplets precipitated were large enough to be detected by a video camera and the precipitation rates and the growth rates were determined from video prints. The droplets first precipitated near the surface of the liquid. The sizes of 10 droplets randomly picked within a snapshot were measured and the measured diameters were averaged. The numbers of the droplets were counted within the same unit apertures randomly selected on the snapshot photos and the averaged number was divided by the area of the aperture to get the density of the droplets, i.e., the density of the nuclei. The nucleation rate and the growth rate are typically measured under an isothermal process. The rates of nucleation and growth given in this study do not correspond to the typical rates but indicate the apparent nucleation rate and the apparent growth rate determined under cooling. The apparent growth rates

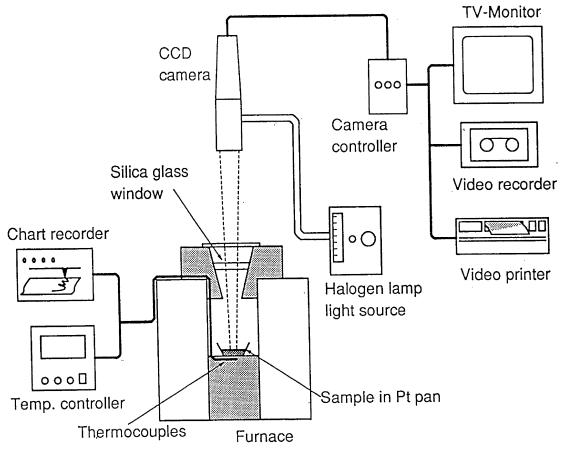

Fig. 2. Block diagram of the setup for the in situ observation of phase separation.

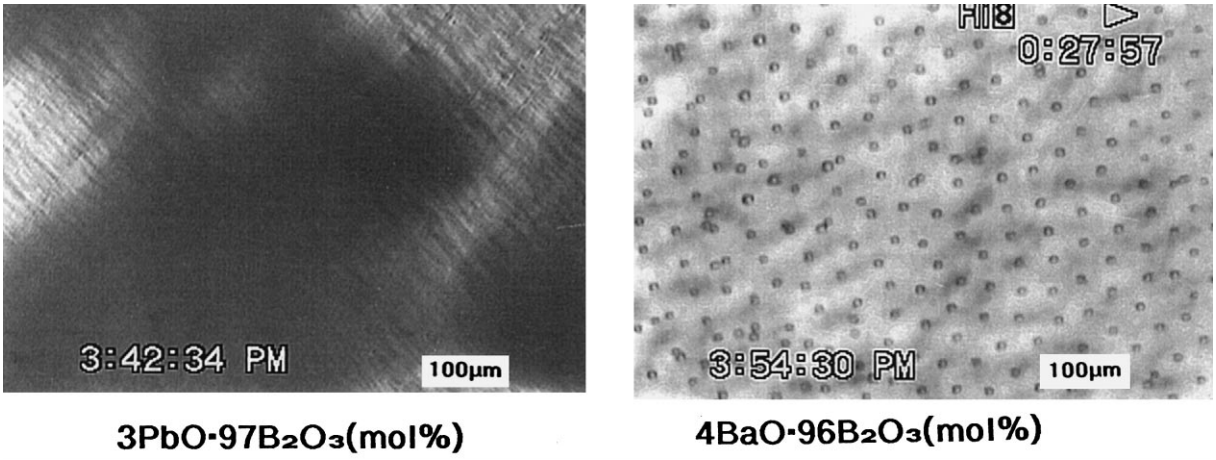

Fig. 3. Video images of the phase separation in $PbO–B_2O_3$ and $BaO–B_2O_3$ system.

were determined from the plots of the sizes of the droplets vs the time elapsed and the apparent nucleation rates were obtained from the plots of the number of the droplets vs time.

The phase separation of the borate melts with added Eu_2O_3 were also observed with the in situ observation setup and the Eu content within droplets was analyzed by scanning electron microscopy equipped with energy dispersion spectrometer (SEM-EDS). Standard samples for determining Eu content in glasses were prepared by adding Eu_2O_3 at 0.5, 1.0 and 1.5 mol% to the base composition $20BaO–80B_2O_3$ (mol%), which corresponds to the composition of the end member of the immiscibility dome [10]. The Eu content of the droplets was determined from a calibration curve in which the intensity of X-ray from Eu in the standard samples was correlated with the nominal Eu_2O_3 content of the standard samples.

Droplets were taken from the phase separated glasses doped with Eu_2O_3 by dissolving the glasses in water, ethanol etc. The solubility of the droplets to these solvents was smaller than that of the matrix, resulting in droplets remaining after the dissolution of the matrix. The fluorescence emission spectra of Eu^{3+} were measured on these droplets using a Raman scattering spectrophotometer equipped with microscope optics, where the excitation wavelength was 465.79 nm from an Ar laser focused onto a droplet.

2.3. In situ observation of phase separation under microgravity circumstances [9]

The drop test facilities that the authors utilized is located in the Micro-Gravity Laboratory of Japan, Toki city, Gifu prefecture, Japan. The drop shaft is 150 m high (100 m for free drop and 50 m for breaking), supplying a 4.5 s duration microgravity environments of $<10^{-5} - g$. The capsule, 900 mm in outer diameter and 2280 mm in height, drops in a vacuum tube of 1.5 m inner diameter.

Fig. 4 shows the block diagram of the set up for the in situ observation of phase separation. The melt of $4BaO–96B_2O_3$ (mol%) was held as a film on a Pt wire (0.5 mm in diameter) loop of about 3 mm in outer diameter. A sample glass flake was placed on the Pt wire loop heated by applying

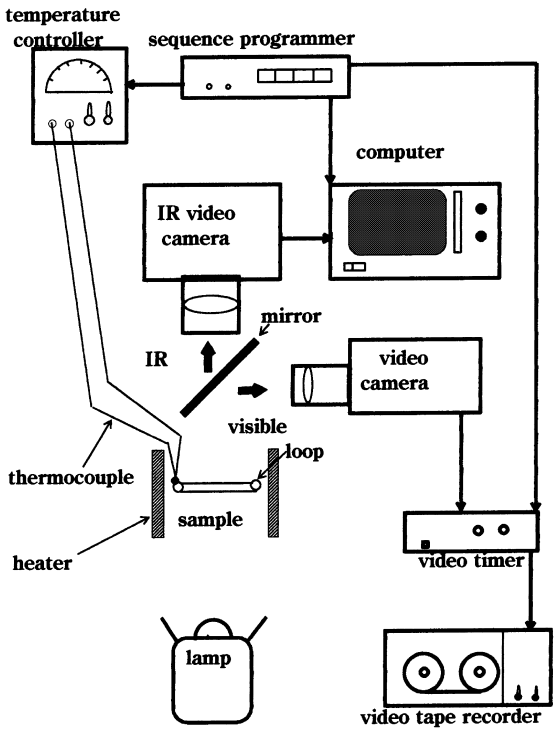

Fig. 4. Block diagram of the setup for the in situ observation of phase separation under micogravity (drop test).

current to the wire and was melted and held as a film on a Pt loop. The thickness of a sample film was estimated to be about 0.5 mm from a calculation in which the mass of the melt was divided by the area of the loop. The Pt loop with a sample film was heated in a Pt wire bobbin heater. The inside of the test chamber including the sample setup was purged with Ar gas. The junction of a Pt–Pt13%Rh thermocouple was welded on the Pt loop to detect the temperature of the sample holding loop. The thermocouple was connected to a temperature controller. The light transmitted through the film was split into visible light and infrared light by a multicoated Si-mirror. The visible light was guided to a video camera to be recorded as video movies. The view field of the video camera is 200 μm in width by 155 μm in height. The infrared light was introduced into an IR video camera and was converted into the two dimensional thermograph by a computer.

The sample film was initially heated to 10°C above the immiscibility temperature, 1160°C, and

was held for a few minutes to homogenize the melt. After the homogenization stage, the melt was cooled to the starting temperature just below the immiscibility temperature, 1155°C, to stand by for the drop. Immediately after the computer received the drop signal, the output power of the temperature controller was turned off to cool the sample at an appropriate rate. Prior to the drop test, the work of the sequencer was tested by running the sequence program at 1-*g*, in which the phase separation was observed and the image was recorded for the experiment at 1-*g* as the reference.

3. Results

3.1. Phase separation rate at 1-g

3.1.1. $PbO–B_2O_3$ system [7]

The time intervals, *t*, are shown as a function of the PbO content in Fig. 5 along with the immiscibility curve calculated by the procedures described in the literature [12]. The *t* increased in the composition range in both ends of the immiscibility dome, indicating that the phase separation was faster in the middle of the dome than the ends of the dome. In the middle of the dome, the time *t* was less than 200 s, which shows that it would be difficult to freeze the texture including particles of an appropriate size. The compositions near the B_2O_3 rich end of the dome were favored for the application of the phase separation to the preparation of glasses dispersed with fine particles.

3.1.2. $BaO–B_2O_3$ system [8]

The correlation coefficients, *R*, of the linear least square analysis between the number of the droplets within a unit area and time on all the compositions tested were included $0.95 \leqslant R \leqslant 0.98$, and with a linear relationship. The apparent nucleation rates were determined as the slopes of the plots of the number of the droplets vs time and the values of the slopes were averaged on several observation experiments.

The correlation coefficients of the linear least square analysis between the average diameter of the droplets and the square root of time on all the compositions tested were included within 0.95–0.98, indicating linear relationship. The apparent growth rates were determined as the slopes of the plots of the diameters of the droplets vs $(\text{time})^{1/2}$ and the slopes obtained from the experiments on a glass sample were averaged.

The apparent nucleation rates and the apparent growth rates of the phase separation were plotted as a function of the BaO content in Fig. 6. The

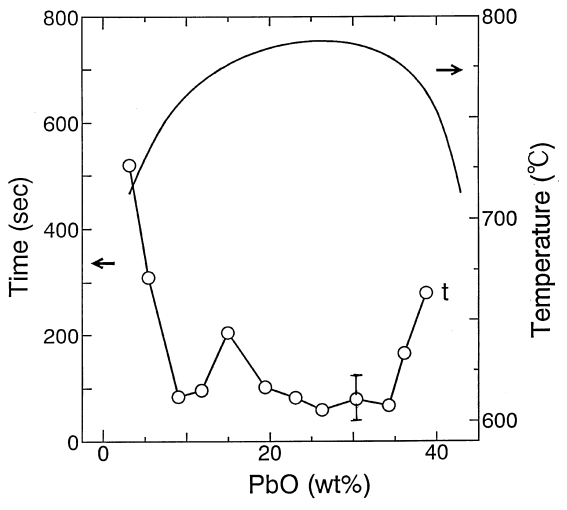

Fig. 5. Dependence of darkening time *t* on the PbO content. The solid line between the data symbols is a guide for the eye.

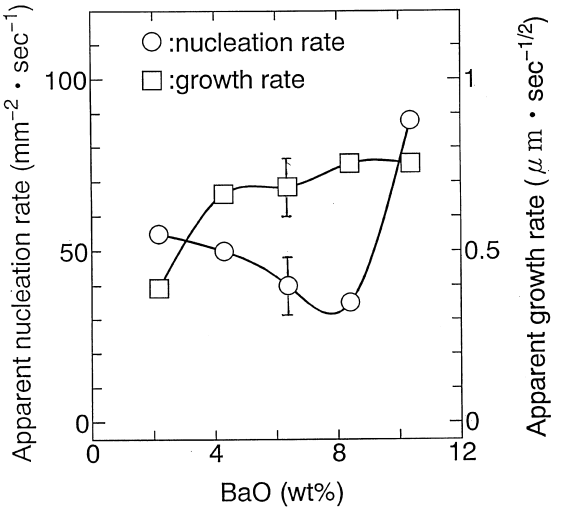

Fig. 6. Apparent nucleation rates and apparent growth rates as a function of the BaO content. Lines are drawn as a guide for the eye.

apparent nucleation rate decreased with the increase of BaO content and showed a minimum around 8 wt% of BaO. The further addition of BaO to the batches from about 8–10 wt% resulted in an increase of the apparent nucleation rate. The apparent growth rate increased with increase of the BaO content. The apparent nucleation rate and the apparent growth rate were about 90 mm^{-2} s^{-1} and 0.9 μm $s^{-1/2}$ at the 10 wt% of BaO, respectively.

The apparent growth rate increased with the increase of the BaO content as seen in Fig. 6. The growth rate is governed by the diffusion rate of the ions [1]. The decrease of the viscosity, which was derived from the increase of the BaO content and the observation temperature [13], would increase the diffusion rate of the ions, resulting in the increase of the apparent growth rate.

Under the conditions employed in this study, the phase separation in $BaO–B_2O_3$ system could be controlled to precipitate of droplets of ~10 μm.

The averaged Eu^{3+} content as Eu_2O_3 within the droplets was about 2.5 times larger than that of the matrix, indicating that the added Eu_2O_3 was concentrated within the droplets.

Fig. 7 shows a typical fluorescence spectrum of Eu^{3+} ions measured on a droplet taken from the droplets left after dissolution of the matrix. The diameter of the droplet observed was 5.0 μm. Some peaks were observed in the ordinary Eu^{3+} emission spectrum in borate glasses which was seen as background of the spectrum in Fig. 7.

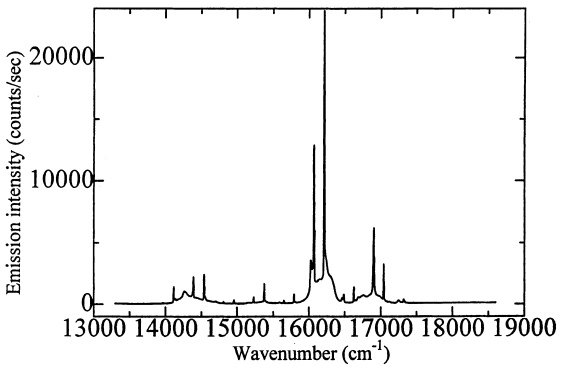

Fig. 7. Emission spectrum of Eu^{3+} measured on a droplet taken out.

3.2. Phase separation under microgravity circumstances [9]

Fig. 8 shows the temperature profiles during the drop test. The central parts of the profiles indicate the temperature at the observed position. The distribution width of the temperature within a loop was estimated to be less than 10°C. The shapes of the profiles were kept almost the same during cooling, indicating that the film was cooled approximately uniformly.

To make the images of the droplets clear, the color snap shots were converted into the black and white images by applying the computer aided image conversion at an appropriate gray scale. The snap shots converted for the microgravity duration time of 0.0, 2.25, 2.5, 3.0, 3.25, 3.5, 3.75 and 4.5 s are given in Fig. 9. The figures showed the precipitation and the growth of the droplets. The droplets precipitated around 2.25 s (corresponding to 1143°C on the thermocouple indication) grew to a few micrometers in diameter at 3.0 s.

The comparison of the separation rates between the drop test and the terrestrial experiments executed for a check of the sequence programs was made qualitatively. The cooling rates in both experiments were equivalent to 4.4°C/s. The precipitation of the droplets at smaller g was delayed by about 1 s behind the timing of the precipitation at 1-g, indicating that the precipitation temperature was less in microgravity circumstances. Moreover

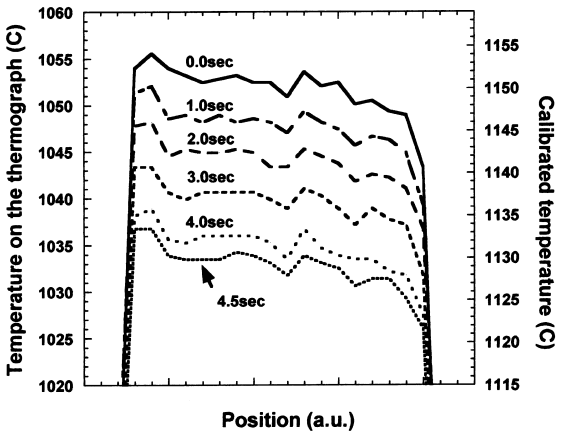

Fig. 8. Temperature profiles on a diameter of the loop with sample melt during drop test.

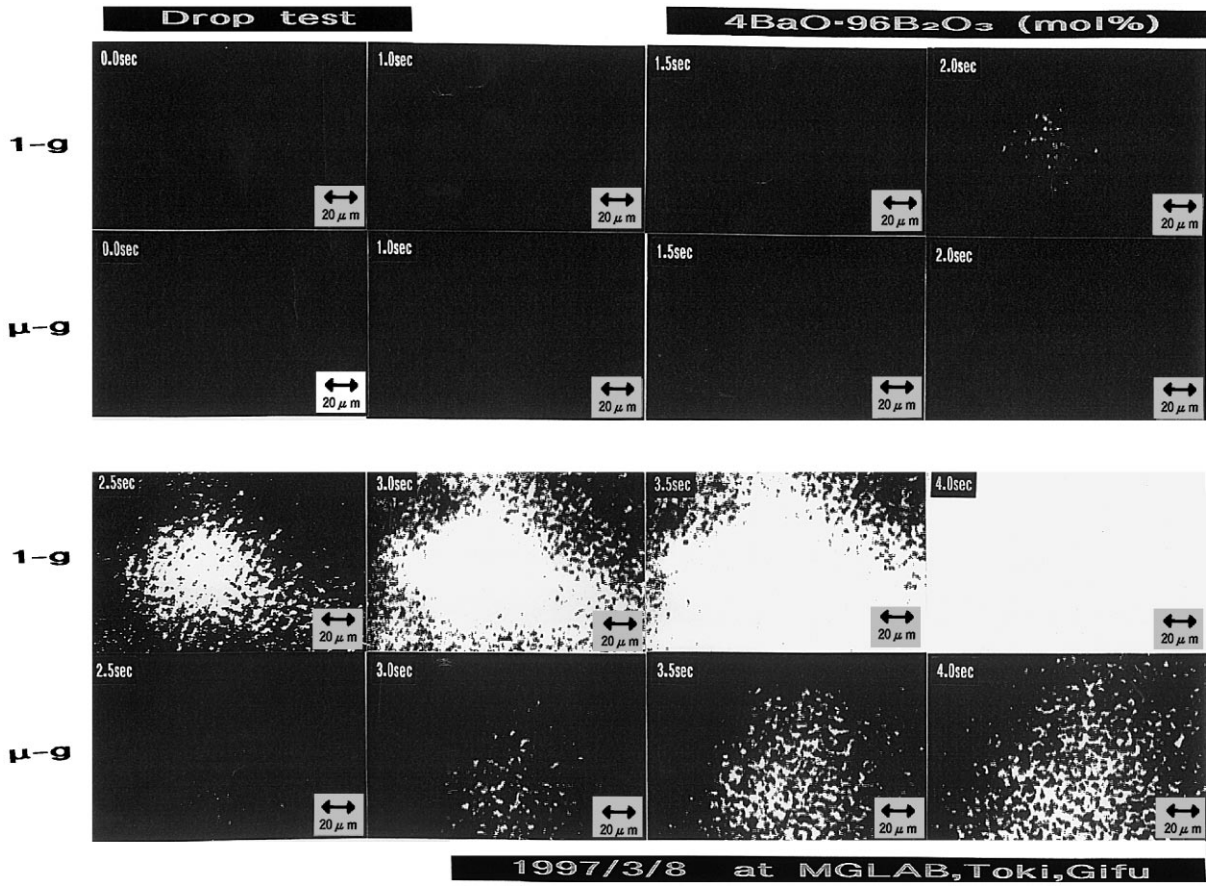

Fig. 9. Black and white images of the video snapshots of the sample melt during drop Test and at 1-*g*.

the rate of the increase of the number of the droplets, corresponding to the nucleation rate, was smaller than that at 1-*g*. We suggest that these results of the comparison show that the phase separation or the precipitation of the droplets was suppressed under microgravity circumstances. The quantitative comparison requires experiments at smaller cooling rates and on compositions giving the smaller population of droplets.

4. Discussion

The precipitation in $PbO–B_2O_3$ system was faster than in $BaO–B_2O_3$ system. The sizes of the precipitated droplets were assumed to be too small to be detected in the video camera. In consideration of the case of $BaO–B_2O_3$ system in which the camera resolved droplets of about 1 μm in diameter, droplets smaller than 1 μm were assumed to be precipitated in $PbO–B_2O_3$ melts. The phase separation near the B_2O_3 rich end of the dome was slower than that in a liquid located in the middle of the dome.

In the $BaO–B_2O_3$ system, precipitation of rather large droplets near the surface of the melts was observed. The spacing between the droplets was almost constant, resulting in a distribution of the droplets on a two dimensional lattice. Fig. 10 shows a photo of a glass sample cooled to room temperature taken through an optical microscope. The square like images observed on the droplets showed the outline of the iris of the optical microscope, suggesting that the droplets worked as lenses.

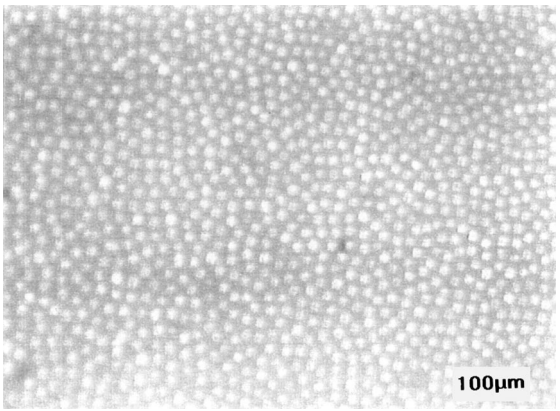

Fig. 10. Optical reflection microscopic photo of the phase separated glass of $3BaO–97B_2O_3$ (mol%).

The wavenumber of the sharp peaks observed on the ordinary Eu^{3+} emission coincided with the wavenumbers calculated for the possible standing wave modes within a glass sphere [14], indicating that the droplets were spherical cavities which enhanced light intensity.

The microgravity circumstances decreased the precipitation rates of droplets in a super cooled borate liquid. The precipitation rate is assumed to derive from the smaller nucleation rate, resulting in a decrease of the number of droplets and precipitating larger droplets. The microgravity duration time was too short to obtain large droplets and thus a comparison of shapes could not be made on the droplets obtained in the drop tests and in the terrestrial experiments. We assume that the weightless condition of the microgravity circumstances assists the precipitation of spherical droplets in the liquids. Therefore the phase separation under microgravity circumstances is favorable for the preparation of the glass spheres containing rare earth oxide and for the glass dispersed with spherical glass particles.

5. Conclusion

In the $PbO–B_2O_3$ system smaller droplets were precipitated than in the $BaO–B_2O_3$ compositions. $BaO–B_2O_3$ system was favorable for preparing glasses dispersed with droplets several tens of micrometer in diameter. The addition of rare earth oxide modified the compositions of the droplets, resulting in an enrichment of the rare earth element within the droplets. The microgravity condition decreased the rate of the precipitation of droplets and would be favorable for the preparation of larger spherical droplets. The photo of the optical reflection microscope of a phase separated glass showed the images where each droplet gave the outline of the iris of the microscope, indicating that the large droplets precipitated could worked as a lens array. Among the processes to form these glasses through phase separation, the feasibility of Processes 1 and 3 has been demonstrated in the borate systems.

References

[1] O.V. Mazurin, E.A. Porai-Koshits, Phase Separation in Glass, North-Holland, Amsterdam, 1984, p. 15.
[2] J. Zarzycki, F. Naudin, Phys. Chem. Glasses 8 (1) (1967) 11.
[3] H.P. Hood, M.E. Nordberg, US patent 221 (1940) 5039.
[4] T. Takamori, M. Tomozawa, J. Am. Ceram. Soc. 59 (9/10) (1976) 377.
[5] R.K. Jain, R.C. Lind, J. Opt. Soc. Am. 173 (5) (1983) 647.
[6] A.F. Witt, H.C. Gatos, M. Lichtensteiger, M.C. Lavine, C.J. Herman, J. Electrochem. Soc. 122 (1975) 276.
[7] S. Inoue, K. Wada, A. Nukui, M. Yamane, S. Shibata, A. Yasumori, T. Yano, A. Makishima, H. Inoue, M. Uo, Y. Fujimori, J. Mater. Res. 10 (6) (1995) 1561.
[8] S. Inoue, K. Wada, A. Nukui, M. Yamane, S. Shibata, A. Yasumori, T. Yano, A. Makishima, H. Inoue, K. Soga, Phys. Chem. Glasses 38 (4) (1997) 197.
[9] S. Inoue, A. Makishima, H. Inoue, K. Soga, T. Konishi, T. Asano, Y. Ishii, M. Koyama, J. Am. Ceram. Soc. 80 (9) (1997) 2413.
[10] E.M. Levin, H.F. McMurdie, J. Res. Nat. Bur. Stand. 42 (1949) 131.
[11] O.V. Mazurin, E.A. Porai-Koshits, Phase Separation in Glass, North-Holland, Amsterdam, 1984, p. 301.
[12] P.B. Macedo, J.H. Simmons, J. Res. Nat. Bur. Stand. A 78 (1) (1974) 53.
[13] O.V. Mazurin, M.V. Streltsina, T.P. Shvaiko-Shvaikovskaya, Handbook of Glass Data. Part B, Elsevier, Amsterdam, 1985, p. 246.
[14] H.C. Van De Hulst, Light Scattering by Small Particles, Wiley, New York, 1957, p. 63.